Grafting Bimodal Polymer Brushes on Nanoparticles Using Controlled Radical Polymerization

ARTICLE *in* MACROMOLECULES · DECEMBER 2012

Impact Factor: 5.8 · DOI: 10.1021/ma3018876

6 AUTHORS, INCLUDING:

Bharath Natarajan
National Institute of Standards and Technology
11 PUBLICATIONS **81** CITATIONS

SEE PROFILE

Linda S. Schadler
Rensselaer Polytechnic Institute
210 PUBLICATIONS **10,243** CITATIONS

SEE PROFILE

Macromolecules

Article

pubs.acs.org/Macromolecules

Grafting Bimodal Polymer Brushes on Nanoparticles Using Controlled Radical Polymerization

Atri Rungta,[†] Bharath Natarajan,[‡] Tony Neely,[†] Douglas Dukes,[‡] Linda S. Schadler,[‡] and Brian C. Benicewicz[†,*]

[†]Department of Chemistry and Biochemistry, University of South Carolina, Columbia, South Carolina 29208, United States

[‡]Department of Materials Science and Engineering, Rensselaer Polytechnic Institute, Troy, New York 12180, United States

Supporting Information

ABSTRACT: RAFT (reversible addition−fragmentation chain transfer) polymerization has been widely used to synthesize different polymer architectures such as polymer brushes on nanoparticles for incorporation into polymer nanocomposites. It is believed that these polymer brushes, with the same chemistry as the matrix polymer, can be employed to improve filler dispersion by compatibilizing unfavorable enthalpic interactions between the inorganic nanoparticles and their organic host matrices. However, monomodal brush graft nanoparticles are found to aggregate into a range of isotropic and anisotropic morphologies, formed due to a delicate balance between enthalpic and entropic interfacial interactions. This coupling of enthalpy and entropy leaves only a small window of graft densities and molecular weights to obtain randomly dispersed filler morphologies. These issues can be countered by using a bimodal polymer brush that contains a small number of long homopolymer chains that can entangle, and a high density of short brushes that screens the particle/particle attraction, thereby aiding in decoupling the interfacial enthalpic and entropic interactions. In the present work, we demonstrate a robust step-by-step technique using RAFT polymerization to synthesize these bidisperse/bimodal polymer brush-anchored nanoparticles. A layer of dense brush of the first population was initially prepared using surface-initiated RAFT polymerization from colloidal silica nanoparticles. After cleavage of the chain transfer agent from the first population of chain ends, a second RAFT agent was attached onto the silica nanoparticles and then a monomer, which may be the same or different from the first brush, was polymerized. This versatile and widely applicable route enables us to independently control the molecular variables of the attached chains, such as composition, molecular weights and graft densities of the individual populations. The bimodal brush-grafted colloidal silica nanoparticles show superior dispersion and interaction with a homopolymer matrix when compared to monomodal brush-grafted particles.

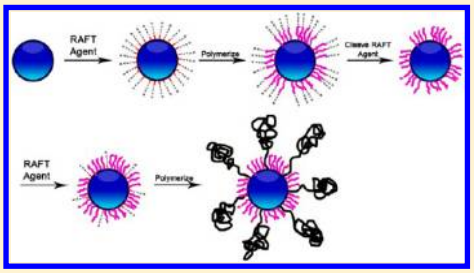

INTRODUCTION

The incorporation of nanoparticles into a polymer matrix has led to the development of materials with new and exciting properties, which are not obtained using micrometer size fillers.[1,2] Often, the interface between the inorganic nanoparticle filler and the organic polymer matrix is critical for obtaining the promised enhancement in properties of the final composite.[3,4] One method of judiciously controlling the interface is to covalently tether polymer chains onto the surface of the nanoparticles. It has been well established in recent years that chemical grafting of a homopolymer brush having the same chemistry as that of the polymer matrix onto the inorganic nanoparticle substrate can potentially alleviate agglomeration and offer improved mechanical properties.[5,6] Experimental and simulation results suggest that high graft density brushes, where $\sigma(N)^{1/2} > 1$ (σ and N being the graft density and degree of polymerization respectively), screen attractive van der Waals interactions between particle cores.[7−9] However, in this graft density regime it is found that even in the absence of a net enthalpic interaction between the brush and matrix, there still remains an unfavorable mean-field entropic surface tension due to *autophobic dewetting* of the matrix from the brush.[7,9,10] This isotropic surface tension leads spherical particles to self-assemble into cubic or close packed aggregates. Autophobic dewetting can be alleviated by reducing the graft density or by increasing the brush to matrix molecular weight ratio.[11,12] However, for a mechanically strong matrix (molecular weight >100 kg/mol), increasing the brush molecular weight reduces the maximum achievable loading of the nanoparticle core, which is essential in preparing functional materials for use in optical, dielectric, and other applications where high nanoparticle loadings are required to obtain large property enhancements.

Decreasing the graft density exposes the particle surface, leading to the self-assembly of fillers into anisotropic string and sheet-like morphologies based on the tethering density of the brush and relative molecular weights of brush and matrix.[12] Anisotropic self-assembly arises because the immiscible particle core and grafted polymer layer attempt to phase separate but are constrained by chain connectivity, analogous to the

Received: September 9, 2012
Revised: November 15, 2012
Published: November 28, 2012

   dx.doi.org/10.1021/ma3018876 | Macromolecules 2012, 45, 9303−9311

behavior of amphiphiles. Akcora et al. developed a morphology diagram through experimentation and Monte Carlo simulation for homopolymer polystyrene-grafted silica composites.[12] The particle cores have a strong short-range attraction, and as they draw nearer, this attraction is countered by the entropic loss involved in distorting the polymer brush chains. The various morphologies are equilibrium structures that result from the minimization of free energy i.e. the balance between short-range enthalpic attraction and long-range entropic repulsion.

Pryamtisyn et al.[13] noted that this "phase-separation" like behavior is strongly dictated by the enthalpic attraction between the filler cores. They defined an interaction parameter capturing the net enthalpic gain per contact: $\chi = (2\varepsilon_{(p\text{-}np)} - \varepsilon_{pp} - \varepsilon_{(np\text{-}np)})/2kT$, where p denotes polymer, np the nanoparticle, and ε is the enthalpic gain in units of kT. In immiscible systems, χ is always positive, and a larger value of χ indicates an increased attraction between cores. The various morphologies were identified by minimizing free energy in different regions of parameter space, resulting from a balance between a dimensionless enthalpic attraction term $\alpha\varepsilon/n_p$ and an excluded volume parameter $\upsilon N^2/R_g^3$. α is a dimensional parameter related to the morphology of dispersion, ε is the enthalpic gain in units of kT, n_p is the number of polymer chains attached per particle, υ is an excluded volume parameter related to the Kuhn length of the polymer and the degree of polymerization of the chain (N) and matrix, and R_g is the radius of gyration of the chain. The simulations found that with increasing enthalpic gain the agglomerated regions of the phase diagram grew at the expense of the dispersed phases. These results suggest that lowering the intercore attraction increases the probability of obtaining well-dispersed systems. We seek to apply this rationale by grafting a bimodal brush with a population of high graft density short chains that reduce the intercore van der Waals attraction and a population of low graft density long chains that enhance excluded volume repulsions.

A bimodal/bidisperse polymer brush is defined as a homopolymer brush with two distinct lengths of monodisperse chains tethered to a surface.[14] When the two polymer species grafted onto the surface are chemically distinct, it is termed a mixed brush. Although single component monodisperse polymer brushes have been successfully grafted onto a range of substrates, including silica nanoparticles using a wide variety of techniques, there are surprisingly few methods in the literature describing the synthesis of binary polymer brush-grafted surfaces. Sidorenko et al. have successfully used a grafting-from approach and a grafting-to approach to prepare binary polymer brushes.[15] Dyer et al. have used a two-step approach to synthesize PMMA and PS mixed brushes on flat silicon substrates.[16] The first brush was polymerized using photochemical initiation from the surface, through a mask in direct contact with the silica substrate. The second brush was polymerized from azo initiators, which were covered by the mask and remained unreacted during the first step. Although these techniques have been successful in making binary brushes, they lack control over important parameters such as molecular weight and graft density. To overcome these limitations, living radical polymerization techniques have been used by Zhao et al. to synthesize mixed polymer brushes.[17] Zhao et al. have made use of an innovative 'Y' shaped initiator with the two arms of the 'Y' initiating consecutive ATRP (atom transfer radical polymerization) and NMP (nitroxide mediated polymerization) reactions. Using this technique they have successfully synthesized responsive poly(acrylic acid)/polystyrene brushes from silica particles and flat silicon wafers.[18] Ye et al. have recently demonstrated a two-step approach based on reverse ATRP, where polymerization is initiated from azo-initiators anchored on the surface of silicon wafers to synthesize mixed brush-anchored substrates.[19] It must be emphasized that all the above brushes have only been grafted on either 150 nm silica nanoparticles or silicon wafers. The effects of varying the graft density and the molecular weight disparity between the chains have not been studied. In addition, studies on hairy nanoparticle colloidal systems are focused primarily on the response of the particles to changes in the environment and not on the properties of nanocomposites they are embedded in. Silica nanoparticles (diameter <100 nm), which have been used extensively in polymer nanocomposite science, have not been functionalized by binary brushes. The techniques to do the same are the focus of the current paper.

We have developed a step-by-step approach to synthesize mixed/binary/bimodal polymer brushes on nanoparticles using the grafting-from approach and RAFT polymerization that is applicable to a large family of monomers and polymer architectures.[20,21] Silica nanoparticles were functionalized with an amine-containing silane that was then reacted with an activated RAFT agent. The first polymerization was conducted using these RAFT-anchored silica nanoparticles. Following the deactivation of the active RAFT agent on the chain ends, a second RAFT agent was attached to the surface of the nanoparticles grafted with the first polymer chain population. The second population of chains can be made with the same monomer or monomers different from the first polymerization. Using this approach, the molecular variables of each chain population can be independently controlled. We demonstrate the importance of decoupling the enthalpic and entropic effects by comparing the dispersion and thermomechanical properties of nanocomposites made from fillers with a single population and a bimodal population of chains.

EXPERIMENTAL SECTION

Materials. Unless otherwise specified, all chemicals were purchased from Fisher Scientific and used as received. Colloidal silica particles (15 nm diameter) were purchased from Nissan Chemical. 2,2′-Azobis(isobutyronitrile) (AIBN) was used after recrystallization in ethanol. Styrene and methyl methacrylate monomers were passed through a basic alumina column to remove the inhibitor before use. Activated 4-cyanopentanoic acid dithiobenzoate (CPDB) was prepared according to a procedure described in literature.[22] 3-Aminopropyldimethylethoxysilane and dimethylmethoxy-n-octylsilane were purchased from Gelest, Inc. and used as received. Highly monodisperse polystyrene (M_w = 96000g/mol; PDI = 1.01), was procured from TOSOH Inc.

Instrumentation. NMR spectra were recorded on a Varian 300 spectrometer using $CDCl_3$ as a solvent. Molecular weights and molecular weight distributions were determined using a Waters gel-permeation chromatograph equipped with a 515 HPLC pump, a 2410 refractive index detector, three Styragel columns (HR1, HR3, HR4 in the effective molecular weight range of 100−5000, 500−30000, and 5000−500000, respectively) with THF as eluent at 30 °C and a flow rate of 1.0 mL/min. The GPC system was calibrated with poly(methyl methacrylate) and polystyrene standards obtained from Polymer Laboratories.

Synthesis of SiO_2-*g*-CPDB. A solution (20 mL) of colloidal silica particles (30 wt % in MIBK) was added to a two-necked round-bottom flask and diluted with 75 mL of THF. To it was added dimethylmethoxy-n-octylsilane (0.1 mL) to improve dispersibility along with 3-aminopropyldimethylethoxysilane (0.32 mL, 2 mmol) and the mixture was refluxed at 75 °C overnight under nitrogen protection. The reaction was then cooled to room temperature and

dx.doi.org/10.1021/ma3018876 | Macromolecules 2012, 45, 9303−9311

Scheme 1. Synthesis of Bimodal Brush Particles Using Step-by-Step RAFT Polymerization

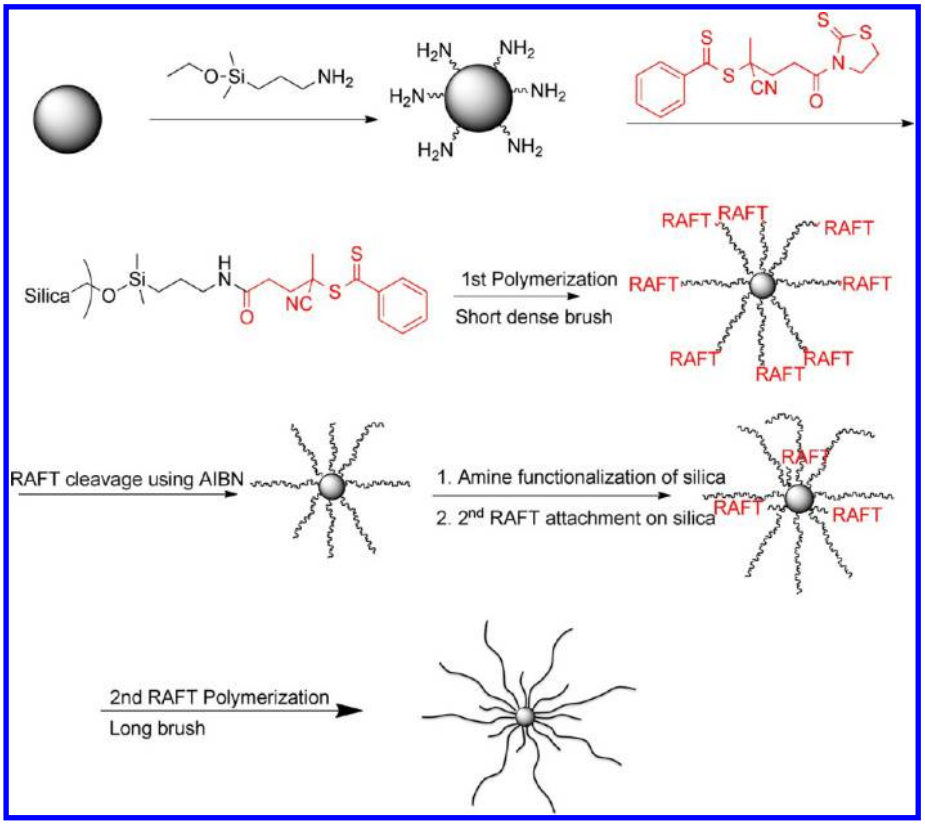

precipitated in a large amount of hexanes (500 mL). The particles were then recovered by centrifugation and dispersed in THF using sonication and precipitated in hexanes again. The amine-functionalized particles were then dispersed in 40 mL of THF for further reaction. A THF solution of the amine functionalized silica nanoparticles (40 mL, 6 g) was added dropwise to a THF solution (30 mL) of activated CPDB (0.67 g, 2.4 mmol) at room temperature. After complete addition, the solution was stirred overnight. The reaction mixture was then precipitated into a large amount of a 4:1 mixture of cyclohexane and ethyl ether (500 mL). The particles were recovered by centrifugation at 3000 rpm for 8 min. The particles were then redispersed in 30 mL THF and precipitated in 4:1 mixture of cyclohexane and ethyl ether. This dissolution−precipitation procedure was repeated 2 more times until the supernatant layer after centrifugation was colorless. The red CPDB-anchored silica nanoparticles were dried at room temperature and analyzed using UV analysis to determine the chain density using a calibration curve constructed from standard solutions of free CPDB.

Graft Polymerization of Methyl Methacrylate from CPDB Anchored Colloidal Silica Nanoparticles to Make SiO_2-*g*-$PMMA_1$. A solution of methyl methacrylate (17 mL), CPDB-anchored silica nanoparticles (1 g, 80 μmol/g), AIBN (1.6 mL of 0.005 M THF solution), and THF (17 mL) was prepared in a dried Schlenk tube. The mixture was degassed by three freeze−pump−thaw cycles, backfilled with nitrogen, and then placed in an oil bath at 60 °C for 3 h. The polymerization solution was quenched in ice water and poured into hexanes to precipitate polymer-grafted silica nanoparticles. The polymer chains were cleaved by treating a small amount of nanoparticles with HF (0.2 mL of a 51% solution in water) and the resulting polymer chains were analyzed by GPC. The polymer cleaved from the SiO_2-*g*-$PMMA_1$ particles had a PDI of 1.07 and a molecular weight of 24400 g/mol which is close to the theoretical value of 26037 g/mol expected for this reaction.

Chain End Deactivation and Cleavage of RAFT Agent from SiO_2-*g*-$PMMA_1$. Solid AIBN (130 mg) was added to a solution of SiO_2-*g*-$PMMA_1$ in THF (1 g by weight of silica in 40 mL THF) and heated at 65 °C under nitrogen for 30 min. The resulting solution was poured into 100 mL hexanes and centrifuged at 8000 rpm for 5 min to recover SiO_2-*g*-$PMMA_1$ nanoparticles. GPC analysis of the cleaved polymer revealed the molecular weight of the polymer was 24200 g/mol and the polydispersity was 1.09.

Functionalization of SiO_2-*g*-$PMMA_1$ by Second RAFT Agent. The second RAFT agent was attached onto the hydroxyl groups of the colloidal silica nanoparticles, which remained unreacted during the first chain immobilization. The bare surface of the nanoparticles was functionalized by amine groups using 0.020 mL of 3-aminopropyldimethylethoxysilane in a process similar to the one described for the first amine functionalization. After the SiO_2-*g*-$PMMA_1$ particles were functionalized by amines, the second CPDB (30 mg) was condensed onto the surface of the nanoparticles to give SiO_2-*g*-($PMMA_1$, CPDB) nanoparticles.

Graft Polymerization of Methyl Methacrylate from SiO_2-*g*-($PMMA_1$, CPDB) to Synthesize Second Brush. The second RAFT agent containing SiO_2-*g*-($PMMA_1$, CPDB) particles (0.3 g by weight of silica) were dissolved in 11 mL THF and added to a dried Schlenk tube along with 11 mL of methyl methacrylate and AIBN (0.19 mL of 0.005 M THF solution). The mixture was degassed by three freeze−pump−thaw cycles, backfilled with nitrogen, and then placed in an oil bath at 60 °C for 12 h after which the polymerization was quenched in ice water. The polymer was recovered by precipitating into hexanes and centrifugation at 8000 rpm. GPC results indicated the second PMMA polymer chain had a molecular weight of 103000 g/mol and PDI of 1.13.

Kinetic Study of Second Chain Polymerization. First 1 g of SiO_2-*g*-(PS_1, CPDB) nanoparticles with a first chain density of 0.2 ch/nm^2 and polystyrene M_n = 7200 g/mol and a second chain density of 0.11 ch/nm^2 (verified via TGA) was dispersed in 40 mL of tetrahydrofuran and then diluted to a total volume of 80 mL in THF. Using a micropipet, six separate Schlenk tubes were prepared with each tube containing 8 mL of nanoparticle solution, 4 mL of styrene, and AIBN (0.060 mL of a 0.005 M THF solution). All tubes were degassed by three freeze−pump−thaw cycles and backfilled with nitrogen. Vial #1 was opened immediately, 1 mL of its contents

dx.doi.org/10.1021/ma3018876 | Macromolecules 2012, 45, 9303−9311

Table 1. Various Bimodal/Mixed Brush-Anchored Silica Nanoparticles Synthesized Using Step-by-Step RAFT Polymerization

number	1st monomer	1st MW, g/mol	1st graft density, chains/nm^2	2nd monomer	2nd MW, g/mol	2nd graft density, chains/nm^2
NP-1	styrene	2000	0.26	styrene	40 000	0.30
NP-2	styrene	3200	0.26	styrene	25 000	0.33
NP-3	styrene	1600	0.26	MMA	205 000	0.07
NP-4	MMA	24 400	0.26	MMA	103 000	0.21
NP-5	styrene	7200	0.18	styrene	119 000	0.047
NP-6*	NA	NA	NA	styrene	100 000	0.05

*Monomodal polystyrene brush-grafted silica nanoparticles.

removed and placed into a preweighed boat, dried, and used as a 0 h comparison for gravimetric analysis. Vials #2−6 were placed into an oil bath at 65 °C and one vial taken out every 12 h. Each vial was quenched in ice water and 1 mL of its contents removed and treated same as vial #1 for gravimetric analysis. All remaining solution in vials #1−6 was separately precipated in hexanes, recovered via centrifugation, and cleaved via HF for GPC analysis.

RESULTS AND DISCUSSION

It is challenging to prepare a bimodal polymer brush with conventional free radical polymerization while maintaining

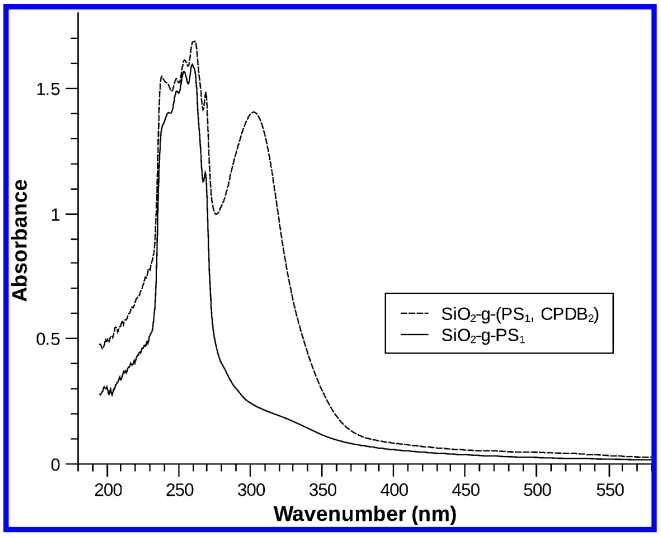

Figure 1. UV absorption spectra of (1) SiO_2-g-PS_1 with cleaved CPDB (solid line) and (2) SiO_2-g-PS_1 with 2nd CPDB immobilized on silica surface (dashed line).

simultaneous control over multiple variables such as grafted chain molecular weight and polydispersity. Using the grafting-from approach and controlled radical polymerization techniques, several groups have previously demonstrated effective methods of synthesizing monodisperse polymer brushes on various surfaces.[21,23−29] We have investigated a method of synthesizing bimodal and/or mixed brush-grafted silica nanoparticles using a step-by-step RAFT polymerization technique (Scheme 1) from surface-anchored chain transfer agents, which we used to synthesize the first population of chains.[16] In this process, a mercaptothiazoline activated-CPDB (4-cyano-4-(phenylcarbonylthioylthio)pentanoate) chain transfer agent was condensed onto the surface of silica nanoparticles functionalized with amine groups. This approach has been used to prepare SiO_2-g-CPDB nanoparticles with graft densities varying from 0.01−0.7 RAFT agents/nm^2 by controlling the ratio of silica nanoparticles to 3-aminopropyldimethylethoxysilane.[21,23−25] An inherent advantage of this technique,

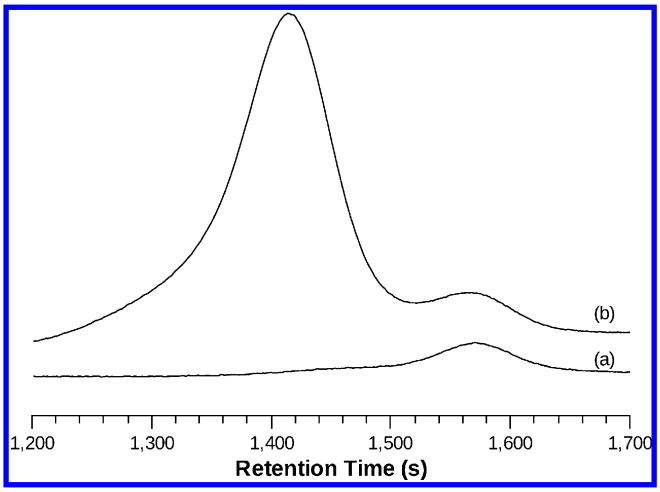

Figure 2. GPC curves of a) first PMMA chains cleaved from SiO_2-g-($PMMA_1$) and b) binary PMMA chains cleaved from SiO_2-g-($PMMA_1$, $PMMA_2$) nanoparticles (NP-4).

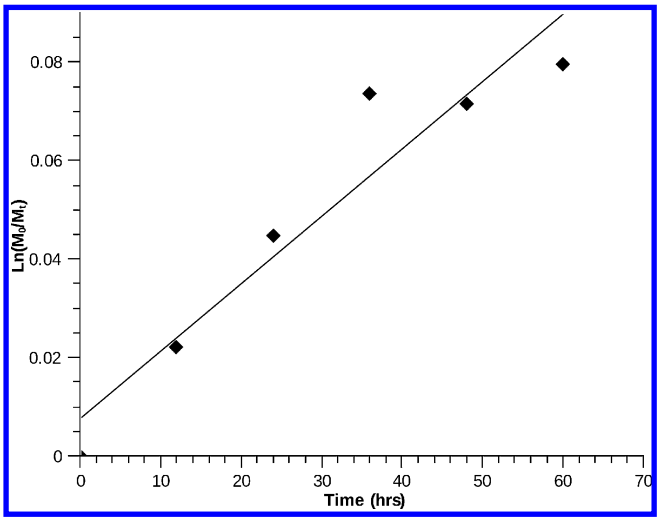

Figure 3. Kinetic plot for polymerization of second population of polystyrene at 0.11 ch/nm^2. First population of polystyrene has graft density of 0.20 ch/nm^2 with molecular weight of 7200 g/mol and PDI of 1.04.

compared to the other grafting-from methods, is the ease and accuracy in measuring the graft density prior to polymerization. The UV absorption at 302 nm of the SiO_2-g-CPDB nanoparticles is compared to a standard absorption curve made from known amounts of free CPDB to determine the concentration of the RAFT agents attached onto the nanoparticles before polymerization.

To prepare sample NP-4 listed in Table 1, surface-initiated polymerization of methyl methacrylate was initially conducted

dx.doi.org/10.1021/ma3018876 | Macromolecules 2012, 45, 9303−9311

Table 2. Matrix Properties, Silica Content, and Polymer Content of Various Nanocomposite Samples Prepared Using NP-5 Bimodal Brush-Grafted Silica Nanoparticles

grafted particle	matrix polymer	silica loading (%)	matrix polymer (%) in composite
SiO_2-*g*-(PS_1, PS_2) particles (NP-5)	PS (M_w = 96000 g/mol, PDI = 1.01)	0	100
		0.1	99.6
		0.5	98.2
		1	96.4
		3.0	89.2
		5.0	81.9
		10	63.8
		25	9.55
		31	0
SiO_2-*g*-(PS_1, PS_2) particles (NP-5)	PS (M_w = 190000 g/mol, PDI = 1.01)	0	100
		0.1	99.6
		0.5	98.2
		1	96.4
		5	81.9
SiO_2-*g*-(PS_2) particles (NP-6)	PS (M_w = 96000 g/mol, PDI = 1.01)	0	100
		5.7	90
		11.5	70
		23.1	50
		35.5	25
		39	0

from the surface of the CPDB immobilized colloidal silica nanoparticles (SiO_2-*g*-CPDB) to give poly(methyl methacrylate) brush-anchored silica nanoparticles (SiO_2-*g*-$PMMA_1$). Azobis(isobutyronitrile) was used as the initiator for the polymerization. A 10:1 [CTA]/[AIBN] ratio was utilized for all polymerizations. The PMMA chains were etched from the SiO_2-*g*-$PMMA_1$ nanoparticles by dissolving an aliquot (50 mg) of the nanoparticles in 4 mL THF and stirring overnight in 0.2 mL HF. Upon evaporation of the THF and HF, the molecular weight of the etched polymer measured by GPC was 24400 g/mol with a polydispersity of 1.07, which agreed with the theoretical molecular weight and indicated control over the polymerization.

Chain End Deactivation. Prior to attachment of the second chain transfer agent, it was necessary to cleave the first chain transfer agent, which remained as an end group from the first polymer population, as a consequence of the first RAFT polymerization. This was achieved using a process similar to that described earlier in literature.[30] Although these techniques have been successfully applied to cleave chain transfer agents from RAFT synthesized homopolymers and copolymers, the removal of a chain transfer agent from a polymer brush has not yet been reported. In this work, chain end deactivation was achieved via a radical cross coupling mechanism using AIBN. However, reducing the AIBN:CTA ratio to 10:1 from 20:1 led to an efficient cleavage reaction and prevented nanoparticle agglomeration. The molecular weight and polydispersity of the polymers before the RAFT cleavage reaction were 24400 g/mol and 1.07 respectively, while after the RAFT cleavage reaction they were 24200 g/mol and 1.09. SiO_2-*g*-$PMMA_1$ nanoparticles appeared pink in color before the cleavage reaction when the RAFT agent was still attached to the polymer. After the cleavage reaction with AIBN, the pink color disappeared to give white polymer coated nanoparticles, which were easily dispersed in THF. The presence or absence of CPDB on silica nanoparticles is easily detected by UV spectroscopy, as shown in Figure 1 for PS grafted nanoparticles.

Attachment of the Second RAFT Agent. Immobilization of the second RAFT agent on the surface of SiO_2-*g*-$PMMA_1$ nanoparticles was achieved using a similar approach as employed for the first RAFT polymerization. The hydroxyl groups on the surface of the silica nanoparticles that remained unreacted during the first chain transfer agent immobilization were reacted with 3-aminopropyldimethylethoxysilane. The 3-aminopropyldimethylethoxysilane molecule is small and can diffuse to the surface of the silica particles to react with the hydroxyl groups even in the presence of the grafted polymer chains from the first polymer population. The concentration of the amine functional silane was critical in determining the graft density of the second polymer brush. By controlling the weight ratio of the 3-aminopropyldimethylethoxysilane to the SiO_2-*g*-$polymer_1$ brush nanoparticles, we successfully varied the graft density of the second population of chains from 0.07−0.36 ch/nm^2. After functionalization of the SiO_2-*g*-$polymer_1$ nanoparticles with amine silane molecules, activated-CPDB was attached to the silica nanoparticles by means of a condensation reaction between the mercaptothiazoline activated-CPDB and the amine groups on the silica surface. The activated-CPDB was used in slight excess (1.4:1) relative to the amine to ensure complete conversion of the amine groups to RAFT chain transfer agents. These CPDB functionalized nanoparticles were washed several times by precipitation in a 4:1 mixture of hexanes and ether and redispersed in THF to remove unreacted CPDB.

RAFT Polymerization of Methyl Methacrylate for Second Polymer Brush Population. Following the immobilization of the second CPDB chain transfer agent on the surface of SiO_2-*g*-$PMMA_1$ nanoparticles to generate SiO_2-*g*-($PMMA_1$, CPDB) grafted nanoparticles, the surface-initiated RAFT polymerization of methyl methacrylate was conducted to give bimodal brush-anchored silica nanoparticles. Methyl methacrylate monomer can easily diffuse to the surface of the silica even in the presence of polymer chains to react with the chain transfer agent after initiation. A monomer to chain transfer ratio in excess of 10000:1 was used to keep the conversion low (under 20%) and avoid gelation, while ensuring the formation of high molecular weight polymer. The molecular weight and polydispersity of the second population of polymer chains, measured by GPC, were 103000 g/mol and 1.13, respectively, indicating excellent control over the second polymerization also. The GPC trace of the cleaved polymer chains from the bimodal nanoparticles is shown in Figure 2b, and is compared to the GPC trace obtained from the first polymer brush (Figure 2a).

The step-by-step RAFT polymerization approach described above was then used to prepare several different types of binary polymer brush-anchored silica nanoparticles as described in Table 1. Bimodal polystyrene graft nanoparticles were synthesized where the polymer composition of both the chains remained the same but the molecular weight of the two populations was varied. For polystyrene, a short dense brush was polymerized at 0.2 ch/nm^2 with a molecular weight of 7200 g/mol and PDI of 1.04. Using these particles, a second polystyrene brush population was polymerized at a density of 0.11 ch/nm^2 under controlled radical polymerization conditions with molecular weights up to 83000 g/mol and polydispersities less than 1.3. The kinetic curve for these

dx.doi.org/10.1021/ma3018876 | *Macromolecules* 2012, 45, 9303−9311

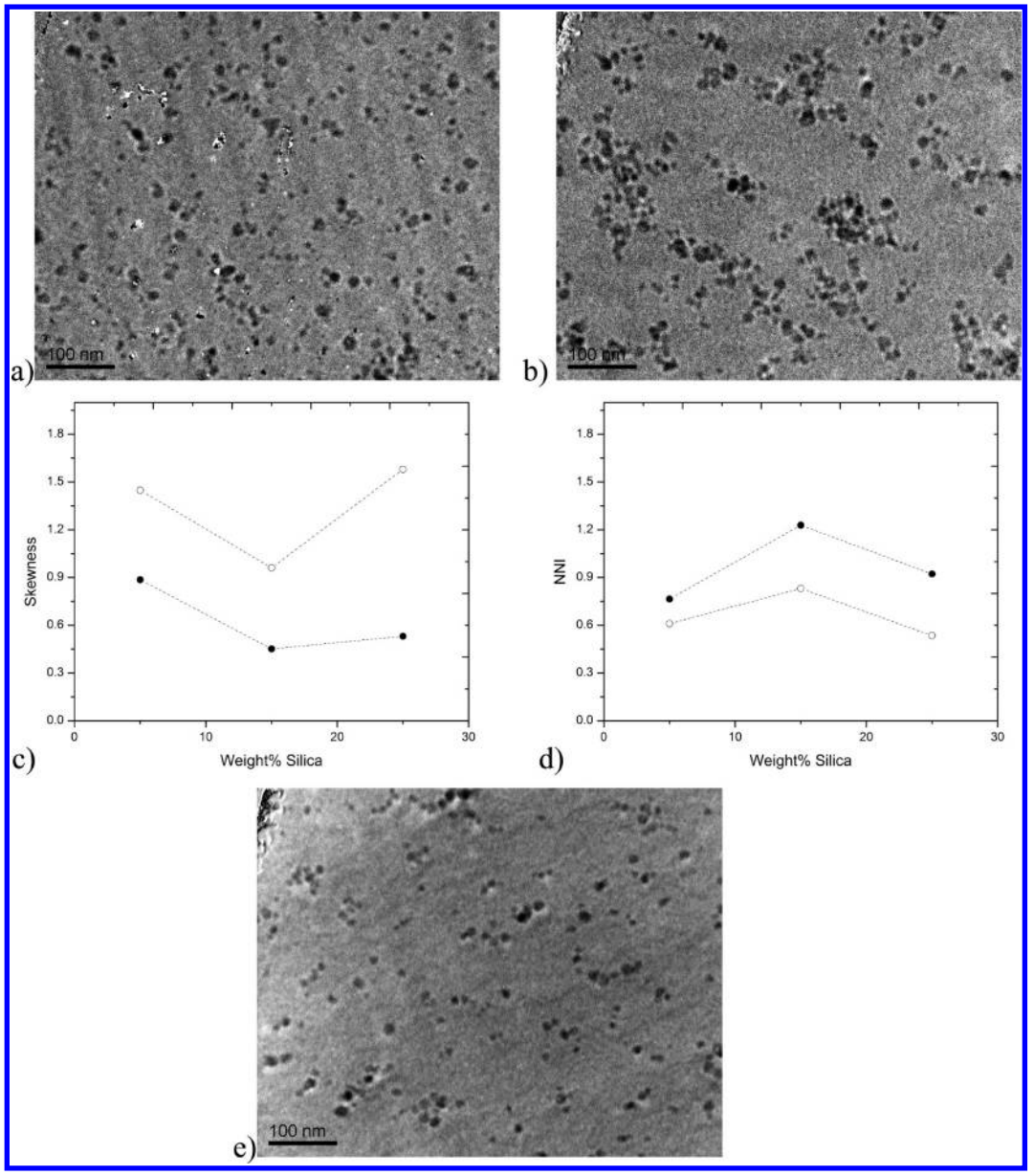

Figure 4. TEM micrographs (at 200000× magnification) of (a) 5% silica loading of NP-5 in 96000 g/mol monodisperse matrix and (b) 5% silica loading of NP-6 in 96000 g/mol monodisperse matrix. (c) Plots of skewness and (d) nearest neighbor index obtained from TEM micrographs (at 100000×) for various loadings of bimodal (●) and monomodal (○) brush graft silica in the monomodal 96000 g/mol matrix. (e) 5% silica loading of NP-5 in a 190000 g/mol monodisperse matrix.

polymerizations is shown in Figure 3. Mixed brush-anchored nanoparticles containing polymer brushes of two distinct polymers were also synthesized using this step-by-step RAFT polymerization procedure.

Polymer Nanocomposites Using Bimodal-Grafted Nanoparticles. To study the effect of the bimodal population of grafted polymer chains on the dispersion and properties of nanocomposites, several nanocomposite samples with monomodal and bimodal polystyrene-grafted nanoparticles (NP-6 and NP-5 from Table 1) were prepared and their thermal and mechanical properties investigated. The details of the free polymer weight fraction and silica content of the various composite samples are described in Table 2. Thermogravimetric analysis revealed a silica core weight fraction of 31% and 39% in the bimodal and monomodal samples, respectively. A detailed description of the preparation of the nanocomposite specimens is provided in the Supporting Information. Care was taken to ensure that the monomodal brush-grafted nanoparticles (NP-6) had a long chain with the same molecular weight and graft density as NP-5, such that based on prior work autophobic dewetting was not a concern for composites system prepared using a 96000 g/mol monodisperse polystyrene matrix.[12]

The dispersion of grafted silica nanoparticles was examined using Transmisson Electron Microscopy (TEM) as shown in Figure 4. Quantitative descriptions of dispersions (skewness and nearest neighbor index (NNI)), which are often more sensitive than visual examination, were obtained by analyzing the TEM images taken at 100000×, as described in the literature.[31,32] Skewness measures the asymmetry in the distribution; therefore a higher skewness indicates a poorer dispersion state. The nearest neighbor index is a measure of

dx.doi.org/10.1021/ma3018876 | Macromolecules 2012, 45, 9303−9311

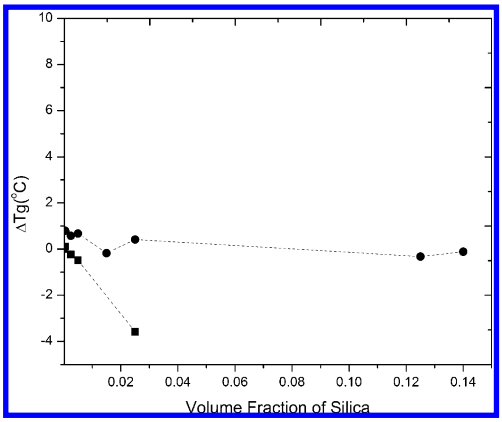

Figure 5. Change in glass transition temperature, T_g for bimodal-grafted NP-5 nanocomposites in 96000 g/mol (●) and 190000 g/mol (■) PS matrixes.

regularity in distribution: NNI > l implies regularity and NNI < l indicates clustering. The larger the departure is from unity, the more significant the regularity or clustering. Parts a and b of Figure 4 show a representative comparison of monomodal and bimodal particle distributions (NP-5 and NP-6) at 5 wt % silica core loading. Parts c and d of Figure 4 are skewness and NNI plots for other silica loadings. It is evident from visual examination of the TEM images and from the plots that the bimodal-grafted nanoparticles disperse more randomly than the monomodal brush-grafted nanoparticles. The monomodal-grafted particles displayed aggregated anisotropic assemblies, which is consistent with the morphologies predicted for this graft density and molecular weight ratio.[8] This is also reflected by the larger skewness and lower NNI values for the monomodal brush systems at these loadings. The improved dispersion in bimodal brush composites is attributed to the addition of short chains, which improves the screening of core/core attraction as suggested by theoretical studies introduced earlier.[9] The NP-5 particles can be envisioned to have a hybrid core with a lowered enthalpic gain per contact χ, but with the same excluded volume advantage as the monomodal long brush. By lowering the enthalpy gain from aggregation, the randomly dispersed morphology becomes the minimum free energy morphology in this parameter space. Note that the bimodal brush-grafted nanoparticles are well dispersed even in a 190000 g/mol polystyrene matrix (Figure 4e).[12]

Thermal Properties of Bimodal Nanocomposite Specimens. The glass transition temperature (T_g) of the bimodal particle filled nanocomposites was measured using differential scanning calorimetry. The temperature was increased at a rate of 10 °C/min from room temperature to 150 °C, held isothermal for 10 min, and then cooled at 10 °C/min to 20 °C. This was repeated three times per specimen. Data from the first cycle was not considered in order to eliminate thermal history effects and the T_g was calculated by averaging the T_g values from the second and third cycles. The calculated T_g values are shown in Figure 5.

Previous work on monomodal nanoparticles composites showed that a matrix of molecular weight larger than that of the grafted brush dewets from the brush resulting in a decrease in T_g due to an excluded volume interaction at the interface.[11] Conversely, the matrix was found to wet the brush at lower molecular weights. The T_g was found to increase in these systems with wetting matrices due to higher matrix-brush friction.[33] Thus, the current T_g data showed a wet to dry transition when the matrix was changed from 96000 g/mol to 190000 g/mol. The 190000 g/mol matrix did not wet the lower molecular weight brush causing a decrease in glass transition temperatures (even with good dispersion), whereas the 96000 g/mol matrix, which was comparable to the brush molecular weight, showed little or no change in T_g. The shift in T_g at 2.5% volume fraction is −3.6 °C for the 190000 g/mol matrix while the shift is 0.5 °C for the 96000 g/mol matrix. These shifts are representative of the dewetting nature of the larger 190000 g/mol matrix, which was observed without any particle agglomeration as would be expected for monomodal systems.[12] We note that these bimodal particles provide the opportunity to isolate wetting and dispersion effects on glass transition temperature, since particles were well dispersed in all systems.

Thermomechanical Properties. Composite samples prepared using the 96000 g/mol polystyrene matrix were processed into dog-bone shaped specimens and subjected to

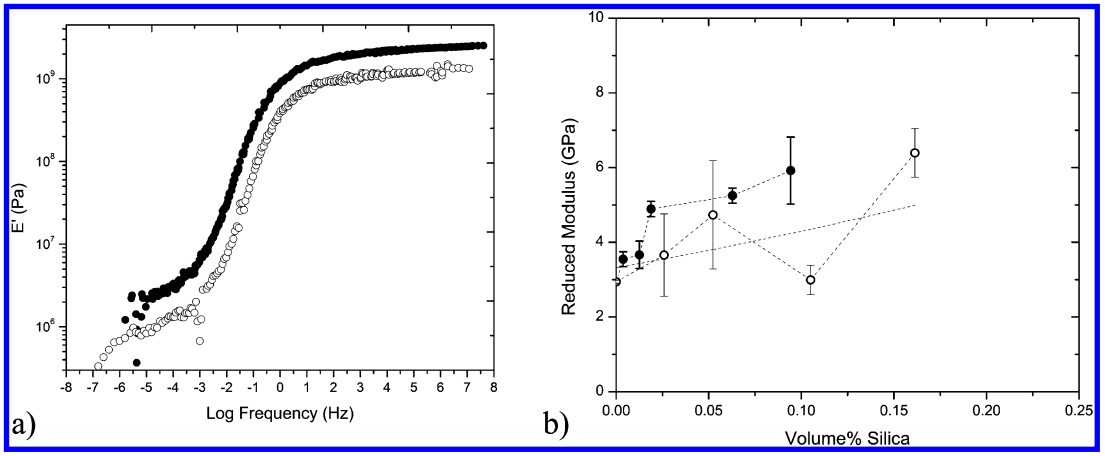

Figure 6. (a) Comparative plot of storage modulus (E') vs log frequency (Hz) for 5% core loadings of bimodal (●) and monomodal (○) brush graft silica in the monomodal 96000 g/mol matrix. The plots are shifted to align T_g to obtain a true comparison of rheological response near the glass transition temperature. (b) Reduced elastic modulus for monomodal- (○) and bimodal-grafted (●) nanoparticle composites measured by indentation, also showing Halpin−Tsai predictions (---). Additionally, frequency sweeps using dynamic mechanical analysis for the 190000 g/mol matrix systems, reveal a steady shift of the normalized loss modulus peaks toward a higher frequency with increased loading as shown in Figure 1s in the Supporting Information. This is in accordance with the decreasing T_g observed on the DSC.

dx.doi.org/10.1021/ma3018876 | Macromolecules 2012, 45, 9303−9311

frequency sweep studies on a Rheometric Scientific DMTA V machine. At this matrix molecular weight, it is expected that the matrix wets the brush reasonably well.[11,33] This is reflected in the T_g data shown in the previous section. Time−temperature superposition was performed on the data using WLF Theory to obtain master curves of the storage and loss moduli.[34] Comparative plots of the storage modulus of identical loadings of colloidal silica core in bimodal and monomodal systems are shown in Figure 6. The bimodal particles displayed a significant improvement in storage modulus over monomodal particles at 5% loading as shown in Figure 6a. The improvement in properties at 5% loading can be explained by the improved dispersion state of the bimodal particles at lower loadings as discussed earlier, as well as the strong entanglement with the matrix. This difference in rheological properties becomes less discernible at high loadings (15%, 25%).

Nanoindentation tests were conducted on the surface of bimodal and monomodal nanocomposite samples. A 150 nm Berkovich diamond tip indentor (Hysitron Company) was used for the test. Hardness and elastic modulii (Figure 6b) of bimodal brush-grafted nanoparticle composites measured by nanoindentation show a remarkable improvement with increasing silica loading. This improvement for bimodal brush-grafted nanoparticles was greater than monomodal brush-grafted nanoparticle composites, particularly at lower loadings and even superior to the values suggested by the Halpin−Tsai mixing rule.[35] We again attribute the enhancement to the excellent dispersion morphology of the nanoparticles and the entanglement with the matrix that causes a physical cross-link. It is also noted that the standard deviation of the hardness and moduli is extremely small in the bimodal systems due to the uniform dispersion of particles. Monomodal nanocomposite samples with agglomerated fillers conversely exhibit large deviations from average values in nanoindentation tests.

CONCLUSIONS

We have developed and demonstrated a robust technique using RAFT polymerization to synthesize binary polymer brush-anchored nanoparticles. A layer of dense brush constituting the first population was initially prepared using surface-initiated RAFT polymerization from silica nanoparticles. The active chain transfer agent at the chain ends was cleaved from the first population of polymer chains using a radical cross coupling reaction. A second RAFT agent was attached to the portion of silica surface not covered by the first chains and was followed by polymerization of a second monomer which could be the same or different from the first brush. This versatile route of using step-by-step controlled polymerization techniques enabled the independent control of the individual molecular variables such as composition, molecular weight, molecular weight distribution and graft density of the two chain populations. The presence of the binary brush was confirmed by GPC traces of the cleaved chains which showed two peaks indicating a bimodal system. TEM analysis of the binary brush-grafted nanoparticles showed that the particles were well dispersed and free from agglomerates. Composites prepared with bimodal brush-grafted nanoparticles showed improved mechanical and thermal properties when compared to monomodal-grafted nanoparticles, due to improved nanoparticle dispersion. The decoupled enthalpic and entropic control over dispersion in these binary/bimodal brush-grafted nanoparticles renders them potentially useful as functional additives in a wide range of applications, such as in smart lighting and stimuli responsive materials.

ASSOCIATED CONTENT

Supporting Information

Text giving details of the transmission electron microscopy, microtoming, and preparation of polymer nanocomposites and a figure showing the dynamic mechanical analysis of bimodal NP-5. This material is available free of charge via the Internet at http://pubs.acs.org.

AUTHOR INFORMATION

Corresponding Author

*E-mail: benice@sc.edu.

Notes

The authors declare no competing financial interest.

ACKNOWLEDGMENTS

This work was supported by the Nanoscale Science and Engineering Initiative of the National Science Foundation under NSF Award Number DMR-0642573.

REFERENCES

(1) Zou, H.; Wu, S.; Shen, J. *Chem. Rev.* **2008**, *108*, 3893−957.
(2) Vaia, R. A.; Maguire, J. F. *Chem. Mater.* **2007**, *19*, 2736−2751.
(3) Schadler, L. S.; Kumar, S. K.; Benicewicz, B. C.; Lewis, S. L.; Harton, S. E. *MRS bulletin* **2007**, *32*, 335−340.
(4) Kumar, S. K.; Krishnamoorti, R. *Annu. Rev. Chem. Biomol. Eng.* **2010**, *1*, 37−58.
(5) Akcora, P.; Kumar, S. K.; Moll, J.; Lewis, S.; Schadler, L. S.; Li, Y.; Benicewicz, B. C.; Sandy, A.; Narayanan, S.; Ilavsky, J.; Thiyagarajan, P.; Colby, R. H.; Douglas, J. F. *Macromolecules* **2010**, *43*, 1003−1010.
(6) Balazs, A. C.; Emrick, T.; Russell, T. P. *Science (New York, N.Y.)* **2006**, *314*, 1107−10.
(7) Ferreira, P. G.; Ajdari, A.; Leibler, L. *Macromolecules* **1998**, *31*, 3994−4003.
(8) Green, P. F.; Oh, H.; Akcora, P.; Kumar, S. K. *Dynamics of Soft Matter*; García Sakai, V., Alba-Simionesco, C., Chen, S.-H., Eds.; Springer: US: Boston, MA, 2012; pp 349−366.
(9) Green, P. F. *Soft Matter* **2011**, *7*, 7914.
(10) Meli, L.; Arceo, A.; Green, P. F. *Soft Matter* **2009**, *5*, 533.
(11) Bansal, A.; Yang, H.; Li, C.; Benicewicz, B. C.; Kumar, S. K.; Schadler, L. S. *J. Polym. Sci., Part B: Polym. Phys.* **2006**, *44*, 2944−2950.
(12) Akcora, P.; Liu, H.; Kumar, S. K.; Moll, J.; Li, Y.; Benicewicz, B. C.; Schadler, L. S.; Acehan, D.; Panagiotopoulos, A. Z.; Pryamitsyn, V.; Ganesan, V.; Ilavsky, J.; Thiyagarajan, P.; Colby, R. H.; Douglas, J. F. *Nat. Mater.* **2009**, *8*, 354−9.
(13) Pryamtisyn, V.; Ganesan, V.; Panagiotopoulos, A. Z.; Liu, H.; Kumar, S. K. *J. Chem. Phys.* **2009**, *131*, 221102.
(14) Skvortsov, A. M.; Gorbunov, A. A.; Leermakers, F. A. M.; Fleer, G. J. *Macromolecules* **1999**, *32*, 2004−2015.
(15) Sidorenko, A.; Minko, S.; Schenk-Meuser, K.; Duschner, H.; Stamm, M. *Langmuir* **1999**, *15*, 8349−8355.
(16) Feng, J.; Haasch, R. T.; Dyer, D. J. *Macromolecules* **2004**, *37*, 9525−9537.
(17) Zhao, B.; He, T. *Macromolecules* **2003**, *36*, 8599−8602.
(18) Li, D.; Sheng, X.; Zhao, B. *J. Am. Chem. Soc.* **2005**, *127*, 6248−56.
(19) Ye, P.; Dong, H.; Zhong, M.; Matyjaszewski, K. *Macromolecules* **2011**, *44*, 2253−2260.
(20) Moad, G.; Rizzardo, E.; Thang, S. H. *Aust. J. Chem.* **2005**, *58*, 379.
(21) Li, C.; Han, J.; Ryu, C. Y.; Benicewicz, B. C. *Macromolecules* **2006**, *39*, 3175−3183.
(22) Mitsukami, Y.; Donovan, M. S.; Lowe, A. B.; McCormick, C. L. *Macromolecules* **2001**, *34*, 2248−2256.

(23) Li, Y.; Benicewicz, B. C. *Macromolecules* **2008**, *41*, 7986−7992.
(24) Dukes, D.; Li, Y.; Lewis, S.; Benicewicz, B.; Schadler, L.; Kumar, S. K. *Macromolecules* **2010**, *43*, 1564−1570.
(25) Maillard, D.; Kumar, S. K.; Rungta, A.; Benicewicz, B. C.; Prud'homme, R. E. *Nano Lett.* **2011**, *11*, 4569−73.
(26) Skaff, H.; Emrick, T. *Angew. Chem.* **2004**, *116*, 5497−5500.
(27) Nguyen, D. H.; Wood, M. R.; Zhao, Y.; Perrier, S.; Vana, P. *Macromolecules* **2008**, *41*, 7071−7078.
(28) Ranjan, R.; Brittain, W. J. *Macromol. Rapid Commun.* **2008**, *29*, 1104−1110.
(29) Pyun, J.; Kowalewski, T.; Matyjaszewski, K. *Macromol. Rapid Commun.* **2003**, *24*, 1043−1059.
(30) Chong, Y. K.; Moad, G.; Rizzardo, E.; Thang, S. H. *Macromolecules* **2007**, *40*, 4446−4455.
(31) Kim, D.; Lee, J. S.; Barry, C. M. F.; Mead, J. L. *Microsc. Res. Techn.* **2007**, *70*, 539−546.
(32) Leggoe, J. *Scr. Mater.* **2005**, *53*, 1263−1268.
(33) Oh, H.; Green, P. F. *Nat. Mater.* **2009**, *8*, 139−43.
(34) Williams, M. L.; Landel, R. F.; Ferry, J. D. *J. Am. Chem. Soc.* **1955**, *77*, 3701−3707.
(35) Halpin, J. C.; Kardos, J. L. *Polym. Eng. Sci.* **1976**, *16*, 344−352.